

D.YU. BALAKIN, YU.G. PTUSHINSKII

Institute of Physics, Nat. Acad. of Sci. of Ukraine  
(46, Nauky Ave., Kyiv 03680, Ukraine; e-mail: dy.balakin@gmail)**ROLE OF FORMATION AND THERMAL  
DESORPTION OF MOLYBDENUM OXIDES  
IN CORROSION OF Mo(110) SURFACE**PACS 68.43.Nr, 68.43.Vx,  
68.47.De, 68.47.Gh

---

*The adsorption interaction of oxygen molecules with the (110) surface of a Mo single crystal at high temperatures has been studied experimentally. The spectra of thermal desorption and the Auger electron amplitude for molybdenum oxides are obtained. The mechanism of corrosion of the Mo(110) surface is found. It is shown that the highest probability of the oxide formation on the Mo(110) surface is attained at a sample temperature of about 1200 K, whereas a further temperature elevation stimulates the process of oxide desorption giving rise to the corrosion.*

*Keywords:* oxygen adsorption, molybdenum oxide, corrosion, temperature-programmed desorption.

**1. Introduction**

The development of the modern space, aviation, and automobile techniques, as well as the chemical industry, needs new anticorrosion and heat-resistant metallic and composite materials. Their application improves the efficiency of technological processes, reduces economic expenses, and prevents emergencies.

Corrosion and electrochemical properties of metals are substantially affected by an oxide layer on the surface. For instance, the properties of nanooxides were used while creating gas sensors [1, 2]. The kinetics of oxide layer formation on metal surfaces is governed by such factors as the electron structure of a metal and the atomic structure of its surface, as well as the composition and the structure of a corrosive medium (the atomic or molecular state of a gas).

Oxygen is one of the most active corrosive agents. Experimental and theoretical researches of initial oxidation stages of Mo(110), W(111), W(110), Pd(100), Pd(111), Rh(110), and Rh(100) surfaces [3–10] showed that the structure of oxides near the surface differs from that in the bulk. In the former case,

the oxide formation is strongly subjected to the diffusion of atomic oxygen into the subsurface layer. As a result, metal atoms entering surface oxide molecules become squeezed between two atomic oxygen layers and form a quasi-two-dimensional surface structure oxygen–metal–oxygen (O–Me–O). This structure cannot be considered as a true oxide nanolayer, but only as a preliminary state for the further formation of a full-blown oxide structure. It was proved experimentally [11–14] that oxygen is not dissolved in the bulk of Mo. Instead, the oxide is formed owing to the oxygen penetration at least into the subsurface molybdenum layer. In work [15], the DFT method was used to calculate the activation energy needed for the oxygen atom to penetrate into the Mo bulk. It equals  $E_a = 4.9$  eV for a perfect Mo(110) surface and  $E_a = 3.5$  eV at the surface step edge. At the same time, the activation energy for the diffusion of an O atom along the surface in the subsurface region amounts only to  $E_a = 0.13$  eV.

The process of oxygen molecule interaction with the (110) molybdenum surface at a low pressure ( $10^{-10}$ – $10^{-3}$  Torr) can be divided into two consecutive stages [11, 13, 16–19]. The first stage includes the dissociative adsorption of oxygen on the molybde-

---

© D.YU. BALAKIN, YU.G. PTUSHINSKII, 2015

num surface (before saturation). On the Mo(110) and W(110) surfaces, oxygen molecules spontaneously dissociate, which results in the oxygen chemisorption even at very low temperatures (45 K) [20]. At the same time, in the case of atomic desorption from adsystems O–Mo(110) and O–W(110), the peak appears at 2000 K, which corresponds to a desorption activation energy of 5.1 eV [11, 13, 17].

The surface saturation with chemisorbed atomic oxygen substantially depends on the specimen temperature  $T_S$ . For instance, at  $T_S = 78$  K, all adsorption centers of the Mo(110) surface became occupied by atomic oxygen at an exposure of 60 L. This fact was established using the molecular beam method and confirmed using the AES one (the Auger peak of oxygen at 507 eV was saturated at 60 L) [17]. A more complete idea of the oxygen adsorption centers on the Mo(110) surface was given in work [21] and, in the case of grooved facets, in work [22] for Mo(112) and [23] for W(112) ones, where the adsorption centers of the following types were described: long-bridge (l-bri), short-bridge (s-bri), with the quasi-threefold symmetry (3-fold), and “on-top”.

The second stage includes the “nucleation” of Mo~O oxide, when oxygen penetrates under the subsurface layer and creates a bond with a neighbor molybdenum atom, which gives rise to the formation of oxide molecules. As their concentration on the surface grows, an oxide layer emerges. Only a small fraction of oxygen molecules that reach the surface (about  $10^{-8}$ – $10^{-5}$ , depending on the specimen temperature) participates in the formation of oxide molecules [17].

The concentration of surface oxides depends on the substrate temperature at the adsorption. Experiments on the thermal desorption of molybdenum oxides allow a quantitative characteristic of this dependence to be obtained. In works [24, 25], the evaporation of oxides was studied by means of the mass-spectrometry detection of evaporation products under quasi-equilibrium conditions, i.e. provided a balance between the numbers of oxygen atoms incident on the surface and departing from it. Owing to reactions on the surface, the chemical nature of incident and departing particles can be different. In particular, at  $T_S > 1600$  K and an oxygen pressure of  $10^{-6}$  Torr, the evaporation of MoO<sub>2</sub> and MoO<sub>3</sub> oxides was observed; whereas, at lower temperatures and high oxygen pressures ( $10^{-5}$  Torr), only (MoO<sub>3</sub>)<sub>2</sub> was detected [25]. Only at high tempera-

tures ( $T_S > 1800$  K), the evaporation of MoO oxide was registered [24].

The thermal stability of oxides is of high importance owing to the development of surface structures with a high selectivity of the catalytic action (e.g., the production of acrylonitrile by oxidizing propylene and ammonia). For instance, Gotoh and Yanokura [7] obtained the surface oxide MoO<sub>2</sub> on the Mo(110) surface at a temperature of 1123 K and an oxygen pressure of  $2.7 \times 10^{-4}$  Pa and showed that MoO<sub>2</sub> is evaporated at a temperature higher than 1373 K. On the other hand, the insufficient stability of oxides can be used for the formation of specific nanostructures with a high surface energy and, hence, a high catalytic activity of their surface. For example, the authors of work [16] established that the MoO<sub>3</sub> oxide quickly evaporates at an annealing temperature higher than 770 K. When the specimens were annealed in the ultrahigh vacuum at 870 K for 20 min, nanostructures with crests were formed.

Our research aimed at studying the characteristic features in the formation of molybdenum oxides on the dense (110) molybdenum surface in the oxygen atmosphere at the surface temperatures  $T_S = 80$ – $2300$  K in order to extend our knowledge about the corrosion of molybdenum and to elaborate recommendations concerning the application of molybdenum in hi-tech processes, such as the soldering of the metal with ceramics, the formation of catalytic surfaces, and the creation of heat-resistant and anti-corrosion coatings.

## 2. Experiment

The experiment was carried out on a high-vacuum installation of the “black chamber” type [26], which allows complex researches of adsorption-desorption processes on a solid surface to be made *in situ*. The application of vacuum chamber walls as a cryogetter deposit allowed us to maintain the pressure of residual gases at a level of  $10^{-10}$  Torr and to make experiments under conditions when particles are detected in the ballistic mode and the background flows of residual gases are efficiently suppressed. The installation was capable of carrying out experiments using the molecular beam (MB), temperature-programmed desorption (TPD) (with the mass-spectrometric detection of particles), low-energy electron diffraction (LEED), and Auger electron spectroscopy (AES) methods. In

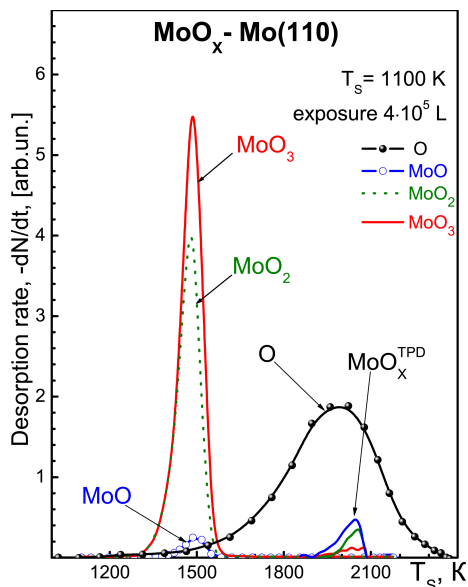


**Fig. 1.** TPD spectrum of the adsystem formed by exposing the Mo(110) surface in the oxygen flow to an expose of  $4 \times 10^5$  L at the substrate temperature  $T_S = 1100$  K. The rate of linear specimen heating  $\chi = 20$  K/s

order to study the oxidized (110) surface of molybdenum, a scanning electron microscope JSM-35 (SEM) was used.

Single Mo(110) crystals with a deviation of their surface from the plane (110) less than  $0.1^\circ$  were used as adsorbents. Molybdenum specimens were cleaned following the standard procedure consisting in a preliminary electrolytic removal of surface contaminations before their mounting in the installation followed by the specimen annealing in the  $O_2$  atmosphere at a pressure of  $1 \times 10^{-6}$  Torr and a temperature of 1600 K with flashes to 2300 K to remove surface oxides [27]. The surface purity was monitored using the AES and LEED methods. The specimen was heated up by bombarding its rear side with an electron beam. The temperature was measured with the help of a WRe5%-WRe20% thermocouple and an optical pyrometer. During the experiments, the specimen temperature  $T_S$  was changed in the interval from 78 to 2300 K. The linear rate of specimen heating  $\chi$  in the TPD method was varied from 0.1 to 40 K/s.

The Auger spectra were measured with the help of a Riber's cylindrical mirror analyzer. The measurements were carried out at the substrate temperature  $T_S = 80$  K and in the following regimes of an Auger spectrometer: the current of a primary elec-

tron beam  $i_p = 80 \mu A$ , the primary electron energy  $E_p = 3000$  eV, and the peak-to-peak modulation voltage  $U_{mod} = 1.2$  V.

An effusive source of oxygen (with a purity of 99.999%) allowed us to obtain a well-collimated molecular beam of  $O_2$  directed immediately to the specimen surface. While forming the oxide layer, the flux of molecular oxygen was varied from  $2 \times 10^{12}$  to  $4 \times 10^{15}$  mol/(cm<sup>2</sup> · s).

### 3. Results and Their Discussion

#### 3.1. Oxide formation on the Mo(110) surface

The temperature-programmed desorption (TPD) spectrum for the system  $MoO_x$ -Mo(110) formed at  $T_S = 1100$  K and exposed in an oxygen flow to a dose of  $4 \times 10^5$  L is depicted in Fig. 1. One can see the desorption of oxides of three types:  $MoO_3$ ,  $MoO_2$ , and  $MoO$ . Their peaks are located in a vicinity of 1500 K, which agrees with the conclusions made in work [13]. The oxide-metal binding energy (3.8 eV) is lower than the oxygen-metal one (5.1 eV). The oxide-metal bond has partially ionic and partially covalent characters. The localization of the external electrons of a metal cation on the oxygen ion weakens the strength of the cation metallic bond with other molybdenum atoms. Hence, a conclusion may be drawn that the oxide formation is associated with substantial spatial and energy reconstructions of bonds between the oxygen and molybdenum atoms on those surface sections, where the "nuclei" of the oxide phase emerge. Owing to these reconstructions, the peaks of molybdenum oxides appear in the TPD mass spectrum at a temperature lower than the temperature of atomic oxygen desorption. A high concentration of  $MoO_3$  in the desorption products in comparison with other molybdenum oxides can be probably resulted from the degree of  $Mo^{+6}O_3^{-2}$  oxidation, which is more beneficial thermodynamically, and the passage of possible surface reactions, which we will consider below.

One can see that the areas under the peaks of oxide molecules are comparable with the area under the peak of atomic oxygen. The processing of those data demonstrates that the number of oxides molecules formed at the given exposure and specimen temperature is approximately four times larger than the number of desorbed oxygen adatoms. As the expose dose increases further, the number of oxide molecules grows even more, unlike the number of oxygen atoms.

The desorption peak of atomic oxygen together with a very insignificant peak of  $\text{MoO}_x^{\text{TPD}}$  oxide is observed at 2000 K. Note that the temperature arrangement of  $\text{MoO}_x^{\text{TPD}}$  peaks (Fig. 1) coincides with that of the atomic oxygen peak, with the saturations of the latter and the oxide peaks being also achieved simultaneously. It is probable that the appearance of the peaks of  $\text{MoO}_x^{\text{TPD}}$  oxides results from the interaction of some oxygen atoms with molybdenum ones and from the formation of molybdenum oxide molecules immediately in the course of oxygen atom desorption at the TPD.

Interesting and important is the issue concerning the correspondence between the thermal desorption spectrum and the actual composition in the oxide nanolayer, as well as whether the appearance of Mo oxides in the thermal desorption spectrum is a consequence of the TPD procedure itself. We tried to find an answer to this question in three ways: with the help of Auger spectroscopy, by determining the reaction order for the desorption of the corresponding oxide, and using the electron microscopy.

In Fig. 2, the Auger spectra of a pure Mo(110) surface with  $T_S = 1100$  K and the same surface but saturated with oxygen to various exposures are exhibited. The saturation of the Mo(110) surface with the chemisorbed oxygen layer stabilizes the amplitude of the oxygen Auger peak (at 507 eV) at exposures of 60 L. One can see that the formation of a chemisorbed layer of oxygen atoms does not give rise to considerable modifications in the Auger peaks of pure molybdenum (at 186 and 221 eV). However, at an exposure of  $4 \times 10^5$  L, the oxygen lines grow, whereas the lines of pure molybdenum disappear almost completely, which is explained by the screening of the Mo surface by a few oxide monolayers (see work [28]). Instead, there emerge Auger peaks in a vicinity of the latter, which are shifted by 5 eV and which obviously correspond to the Auger transitions of the molybdenum atom in the oxide. Our AES results agree with those of work [18], where, besides the Auger spectra from the oxidized Mo(110) surface, important results were also obtained using the HREELS method. The latter showed that the growth of oxides manifested itself in the emergence and the development of a peak at  $740 \text{ cm}^{-1}$ , when the exposure increased to  $10^5$  L. The peak at  $740 \text{ cm}^{-1}$  also testifies that the formation of molybdenum oxide molecules has already started. However, the TPD results [18]

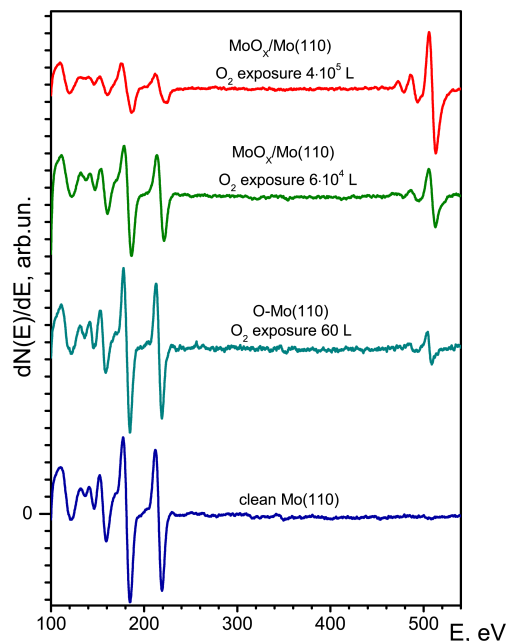


**Fig. 2.** Auger spectra of the Mo(110) surface at various specimen exposures in the oxygen molecular beam. The substrate temperature at the adsorption was  $T_S = 1100$  K. The Auger spectra were measured at a substrate temperature of 80 K

did not reveal the desorption of oxides, because the TPD procedure was carried out only to the specimen temperature  $T_S \leq 1400$  K.

The analysis of the oxide TPD spectra obtained for a specimen saturated with oxygen to various exposures has the following basis. If “ready” compounds are thermally desorbed, we should expect the first order of the thermal desorption reaction ( $n = 1$ ), of which the asymmetric shape of curves and, in the absence of a lateral interaction between adsorbate particles in the adlayer, the independence of the TPD peak position of the coverage degree  $\theta$  are typical. In the case of associative desorption, i.e. when oxide compounds are formed in the course of desorption event, we obtain a reaction of the second order ( $n = 2$ ), of which the symmetric shape of TPD curves is typical, irrespective of the coverage degree; in addition, when  $\theta$  increases, a shift of the TPD peak toward lower temperatures is also observed [27],

$$R = -\frac{dN}{dt} = \nu N^n \exp\left(\frac{-E_d - e_i(N)}{kT}\right), \quad (1)$$

where  $N$  is the surface concentration of oxide molecules,  $n$  the reaction order,  $\nu$  the pre-exponential

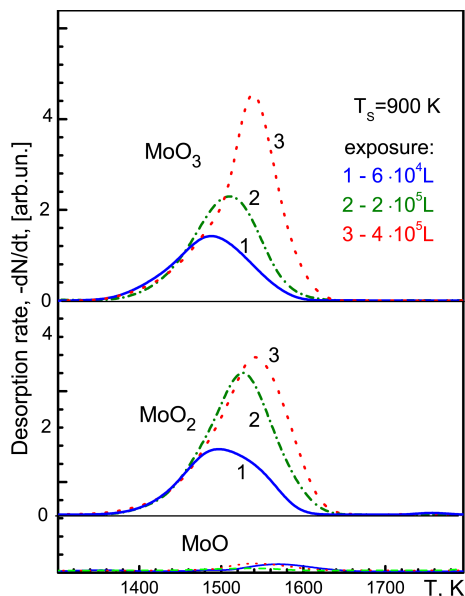


Fig. 3. TPD spectra for oxides at  $T_s = 900$  K and various exposures:  $6 \times 10^4$  (1),  $2 \times 10^5$  (2), and  $4 \times 10^5$  L (3). The rate of linear specimen heating  $\chi = 20$  K/s

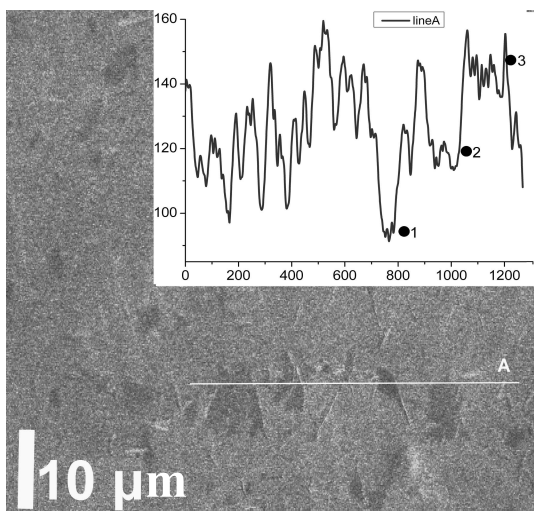


Fig. 4. Image of the oxidized Mo(110) surface formed by secondary electrons at the energy and the current in the primary beam  $E = 32$  keV and  $i = 10^{-11}$  A, respectively. The probing beam width was 10 nm. The pressure in the SEM chamber was  $10^{-5}$  Torr. The intensity of the signal from secondary electrons measured along line A is shown in the inset

frequency multiplier,  $E_d$  the activation energy of particle desorption, and  $e_i(N)$  the energy of the lateral interaction between the molecules in the oxide film. Note that the quantity  $e_i(N)$  is negative in the

case of attractive interaction and positive in the case of repulsive one.

The experimentally obtained TPD spectra were asymmetric for all molybdenum oxides (Fig. 3). They can be described by the Polanyi–Wigner equation for the first-order desorption reaction with regard for the lateral interaction (between the oxide molecules in the formed oxide film), which is an argument in favor of the formation of MoO, MoO<sub>2</sub>, and MoO<sub>3</sub> oxides in the course of adsorption procedure before the TPD one. This conclusion is confirmed by the results of SEM measurements. Figure 4 demonstrates the image of the oxidized molybdenum (110) surface formed at a temperature of 1100 K and an exposure of 4 L; afterward, the specimen was removed from the vacuum installation and immediately examined on a scanning electron microscope. The major factors that affect the signal intensity are the surface relief, work function, and average atomic number  $Z$ . The figure shows that the surface is almost planar, so that the relief weakly affects the signal of secondary electrons. In a rather low vacuum, the formed adsorbed layer compensates, to some extent, the influence of the work function on the intensity of secondary electron emission. In this case, the main factor affecting the output signal of secondary electrons is the average atomic number  $Z$ . According to the results of work [29], this signal grows, as  $Z$  increases. Therefore, the dark sites in the image correspond to smaller averaged atomic numbers in those sections. The latter can probably correspond to islands of the oxidized surface. The inset shows the intensity of the secondary electron signal along scanning line A. At three sections (marked as ●1, ●2, and ●3 in Fig. 4), the intensities are different and discrete. The estimation of the signal intensity allowed us to make assumption that oxides of different types – MoO, MoO<sub>2</sub>, and MoO<sub>3</sub> – were formed on those sections.

Hence, we have ground to assert that the TPD spectrum in Fig. 1 corresponds to a real content of oxides in the film, and oxide molecules are desorbed in the same form, as they had on the surface before the TPD procedure started. The existence of a certain temperature interval, in which oxide molecules are observed to appear and their number grows, can be explained as follows. Oxide “nuclei” Mo ~ O can emerge, when the diffusion coefficients for oxygen adatoms on molybdenum are high enough. Really, as the substrate temperature grows, anharmonic vi-

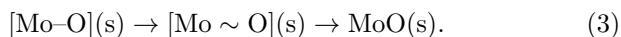
brations of the molybdenum crystal lattice increase, and the probability for oxygen atoms to penetrate under the subsurface layer also increases, which can facilitate a reconstruction of the crystal lattice with the formation, first, of Mo ~ O complexes and, afterward, oxide molecules. At low substrate temperatures ( $T_S \leq 300$  K), the mentioned diffusion coefficients are rather low, and, as a result, oxide “nuclei” do not appear. For instance, our researches [19] showed that the number of oxide molecules formed at  $T_S = 300$  K and an exposure of  $4 \times 10^5$  L is less than 1% of the number of desorbed oxygen atoms. In the case of high temperatures, the diffusion rates for oxygen and molybdenum are sufficient for the probability of the oxide formation to grow, as was observed at temperatures of 700–1250 K. However, if the substrate temperature is too high ( $T_S > 1250$  K), the evaporation of oxides becomes the dominating process.

Let us present some additional speculations concerning the formation of a composition of the oxide nanolayer. For this purpose, we have to consider the possible elementary processes that occur at collisions of O<sub>2</sub> molecules with the molybdenum surface. One of those processes is the dissociation of an O<sub>2</sub> molecule into atoms. This process can be described by the schematic formula



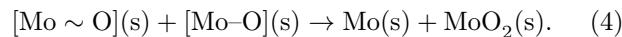
Hereafter, while describing the elementary processes, particles that arrive at the surface from the gas phase or are desorbed from the surface into the gas phase are denoted as (g), whereas particles on the surface as (s).

Chemically active oxygen atoms that appear on the molybdenum surface as a result of the dissociation (2) can penetrate into the subsurface layer to form “nuclei” of Mo ~ O oxide, which either transform into oxide molecules or react with other oxygen atoms and molecules depending on their lifetime on the surface, the specimen temperatures, and the desorption activation energy,

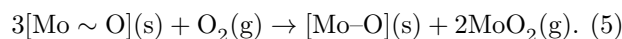


However, according to Fig. 1, process (3) has a low probability, because the number of MoO molecules on the molybdenum surface is insignificant.

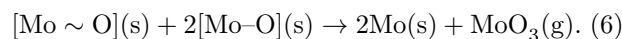
MoO<sub>2</sub> molecules can be formed according to the reaction



In the case where  $T_S > 1300$  K, the incident O<sub>2</sub> molecule (from the gas phase) can interact with the molybdenum surface according to the process



MoO<sub>3</sub> molecules can appear provided the long lifetime of a Mo ~ O oxide “nucleus” and its interaction with the functional group Mo–O (chemisorbed oxygen), when  $T_S < 1600$  K:



If  $T_S > 1300$  K, the MoO<sub>3</sub> molecule can be formed due to the interaction between the O<sub>2</sub> molecule and the oxide “nucleus” Mo ~ O:



At high enough temperatures ( $T_S \gg 1300$  K), those molecules are evaporated into the gas phase, and the inverse reactions to the oxidation level Mo<sup>+6</sup>, which is more beneficial thermodynamically, become feasible:



The presented sequence of processes (2)–(8) makes it possible to explain the appearance of all experimentally observed oxides on the molybdenum surface. Therefore, we arrive at a conclusion that the content of oxides is governed by the following processes: the particle exchange between the layer of atomic oxygen, on the one hand, and the adsorbent and oxide atoms on the molybdenum surface and oxygen in the gas phase, on the other hand; inverse surface chemical reactions: transformations of one oxide molecules into others; and evaporation of oxide molecules and atomic oxygen from the molybdenum surface.

### 3.2. Probability of the formation of oxide molecules

The efficiency of oxide layer formation depends on the specimen temperature  $T_S$ , at which the surface undergoes the oxidation. On the basis of experimental data, the probability of the formation of oxide molecules in

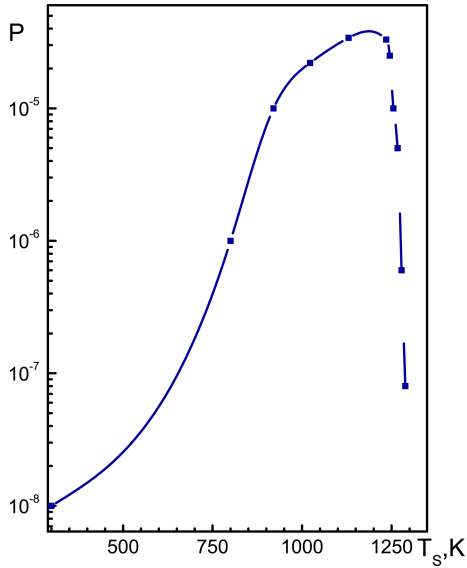


**Fig. 5.** Dependence of the probability of the oxide layer formation on the substrate temperature

the oxide nanolayer and its dependence on the substrate temperature,  $P(T_S)$ , were calculated. For this purpose, we, first, carried out an experiment on the oxygen adsorption on a molybdenum surface at various substrate temperatures  $T_S$ 's, keeping an exposure of  $1 \times 10^5$  L to be constant throughout the experimental series. After the required exposition of the specimen in the oxygen flow, the latter was blocked, and the TPD procedure was executed with the linear heating rate  $\chi = 20$  K/s. The obtained TPD spectra were used to calculate the probability of the formation of oxide molecules with regard for all molybdenum isotopes and the difference between the ionization probabilities for molecules of different molybdenum oxides in the ionic source of a mass-spectrometer:

$$P(T_S) = \frac{1}{F t A} \int \left( 0.5 \frac{dN_{\text{MoO}}(T_S)}{dt} + 1 \frac{dN_{\text{MoO}_2}(T_S)}{dt} + 1.5 \frac{dN_{\text{MoO}_3}(T_S)}{dt} \right), \quad (9)$$

where

$$N_{\text{MoO}_x} = \int \sum_{k=1} \Lambda_x^k I_{\text{MoO}_x}^k = 4.2 \Lambda_x \int I_{\text{MoO}_x}^{\text{reg}} dt, \quad (10)$$

$F$  is the flow of oxygen molecules;  $t$  the adsorption time;  $A$  the substrate area;  $N_{\text{MoO}}$ ,  $N_{\text{MoO}_2}$ , and

$N_{\text{MoO}_3}$  are the numbers of the corresponding oxide molecules formed at a fixed  $T_S$ ; and  $I_{\text{MoO}_x}^{\text{reg}}$  is the ionic current created by the molecules of  $\text{MoO}_x$  oxide in the ionic source of a mass-spectrometer. The coefficient 4.2 was introduced into Eq. (10) to account the isotopic composition of Mo, and the coefficients  $\Lambda_{1,2,3}$  to account the difference between the ionization probabilities of molecules of different oxides in the ionic source of a mass-spectrometer.

As a result, we obtained the dependence of the probability for an oxygen molecule to be captured into the oxide state on the specimen temperature  $T_S$ . This dependence is depicted in Fig. 5. It has a characteristic maximum. At low temperatures,  $T_S \leq 1200$  K, the probability of the oxide molecule formation on the Mo(110) surface increases, as  $T_S$  grows, from  $10^{-8}$  to a maximum value of  $10^{-5}$ . The highest probability of the oxide formation on the surface is reached at a specimen temperature of about 1200 K. If the specimen temperature grows further, despite that the probability of the formation of oxide molecules in the presence of oxygen molecules increases, the efficiency of the oxide nanolayer formation drastically falls down as a result of the oxygen molecule desorption. Therefore, the temperatures  $T_S = 900 \div 1200$  K are optimal for the formation of an oxide nanolayer on the Mo(110) surface. Note also that the lateral forces between oxide molecules that act on the substrate surface are attractive, which enhances the thermal stability of the oxide layer for higher coverage degrees [17].

### 3.3. Corrosive destruction of the Mo(110) surface

The role of oxygen in the formation of molybdenum oxides and the corrosive surface destruction was established on the basis of experimental results obtained under the conditions of a permanent flow of oxygen molecules within the interval  $F = 10^{12} \div 10^{15}$  mol/(cm<sup>2</sup> · s) and  $T_S > 1200$  K. Under those conditions, the adsorption and the dissociation of O<sub>2</sub> molecules occur permanently and simultaneously with the formation and the desorption of oxide molecules and oxygen itself. In Figs. 6 and 7, the dependences of the evaporation intensity on the substrate temperature are shown for three types of oxide molecules and various oxygen flows. One can see that the desorption products contain the same molecules

of molybdenum oxides that form the oxide layer (see Fig. 1).

The increasing sections of the curves in Fig. 6 testify to the activation mechanism of oxide formation. The rate of oxide molecule formation is substantially affected by the diffusion of oxygen atoms into the subsurface layer, which grows, as the temperature of the latter,  $T_S$ , increases. However, an elevation of the specimen temperature reduces the equilibrium concentration of chemically active atomic oxygen, since its lifetime on the surface decreases, and it is desorbed. The formation of  $\text{MoO}_3$  molecules becomes less probable at a considerable deficiency of atomic oxygen on the surface; however, its amount is sufficient for the formation of  $\text{MoO}_2$  molecules and, all the more so,  $\text{MoO}$  ones. The temperature dependences are characterized by the presence of maxima: the larger the number of oxygen atoms in a molecule, the lower is the temperature, at which the maximum is attained. For instance, a  $\text{MoO}_3$  molecule contains less bonds with other substrate atoms; therefore, the desorption activation energy for  $\text{MoO}_3$  (3.5 eV) is lower than for  $\text{MoO}_2$  (4.4 eV) and  $\text{MoO}$  (5.4 eV).

Demonstrative are the results obtained when the oxygen flow increases from  $4 \times 10^{12}$  to  $8 \times 10^{14}$  mol/(cm<sup>2</sup> · s) (Fig. 7). The equilibrium concentration of atomic oxygen at the surface grows at that, and the probability of the formation of oxides with a higher oxygen content ( $\text{MoO}_3$ ) also grows. It is also easy to explain, at the qualitative level, a shift of the curve maxima toward higher temperatures observed for molecules with lower contents of oxygen atoms (Fig. 7). The circumstance that the  $\text{MoO}_3$  molecule is desorbed first stems from the fact that the transition to  $\text{Mo}^{+6}\text{O}_3^{-2}$  is thermodynamically beneficial, and the corresponding sublimation temperature is lower than for other oxides. As the substrate temperature increases ( $T_S > 1400$  K), the lifetime of oxygen adatoms on the surface decreases, and the formation of  $\text{MoO}_3$  becomes hardly probable (the molecule has no time to be formed), because the desorption of  $\text{MoO}_2$ ,  $\text{MoO}$ , and  $\text{O}^*$  begins. Hence, the content of desorption products is determined by the equilibrium constants for the reversible surface chemical reactions (7) and (8) and by the evaporation rates of oxide molecules and oxygen.

Similar dependences of the evaporation rate of  $\text{MoO}_2$  and  $\text{MoO}_3$  oxides on the substrate temperature (with the maxima at 2000 and 1750 K, respec-

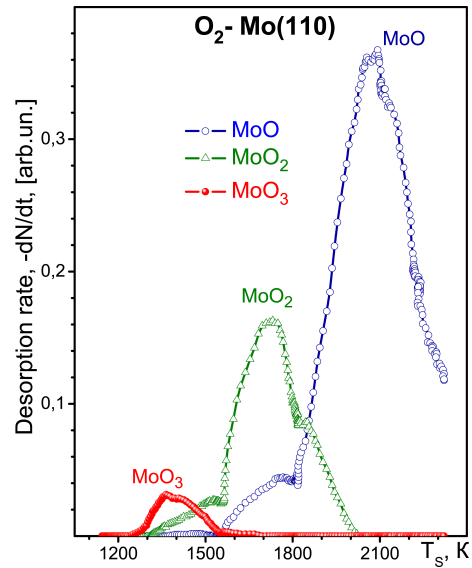


Fig. 6. Dependences of the evaporation rates for various molybdenum oxides from the Mo(110) surface on the substrate temperature  $T_S$  at a constant oxygen flow to the examined surface,  $F = 4 \times 10^{12}$  mol/(cm<sup>2</sup> · s). The rate of linear specimen heating  $\chi = 20$  K/s

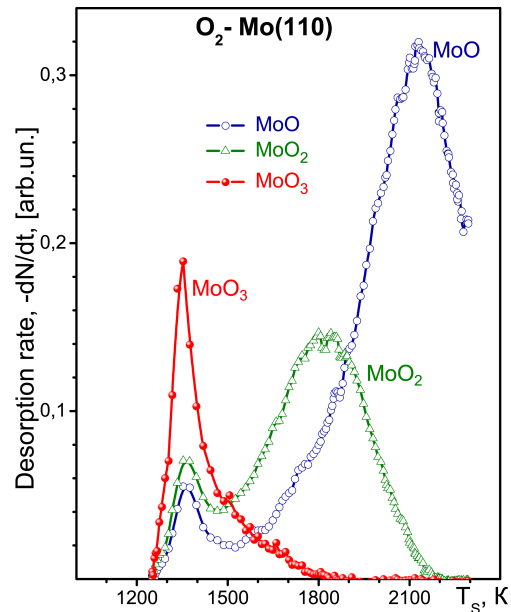


Fig. 7. The same as in Fig. 6, but for  $F = 8 \times 10^{14}$  mol/(cm<sup>2</sup> · s)

tively) at the oxygen pressure  $P_{\text{O}_2} = 1 \times 10^{-3}$  Torr were obtained by Berkowitz-Mattuck *et al.* [24] for polycrystalline molybdenum and tungsten. However, molybdenum monoxide ( $\text{MoO}$ ) was not observed

for the polycrystalline specimen at any temperature.

Hence, the corrosion intensity on the Mo(110) surface grows as the specimen temperature and the oxygen flow (pressure) increase. The composition of oxides and their relative concentrations change together with the equilibrium concentration of oxygen adatoms on the surface, which depends on the temperature  $T_S$ . The relative concentrations of oxides change with increase of the specimen temperature  $T_S$  in such a way that the fraction of oxide molecules with a smaller number of oxygen atoms is larger.

#### 4. Conclusions

The formation and the evaporation of molecules of molybdenum oxides is a corrosive destruction of the molybdenum surface. The presented results contain information concerning the role of molybdenum oxide molecules of each sort in the corrosion process. Irrespective of the number of oxygen atoms in the oxide molecule, the latter, at desorption, captures one molybdenum atom from the surface and, in such a manner, destroys it.

The molecule of molybdenum oxide is formed, when a chemically active oxygen atom penetrates under the subsurface layer of molybdenum atoms (at  $T_S > 700$  K), changes the spatial structure and the binding energies between the oxygen and molybdenum atoms, and creates an oxide “nucleus”  $\text{Mo} \sim \text{O}$ . Just this “nucleus” chemically reacts with adsorbed oxygen to form an oxide molecule:  $\text{MoO}$ ,  $\text{MoO}_2$ , or  $\text{MoO}_3$ . All types of molybdenum oxides begin their formation simultaneously, and their concentrations grow, as the exposure increases. At first, oxides form surface structures (clusters); then, as their concentrations grow, an oxide layer, owing to the attractive lateral interaction between the oxide molecules. The formed surface structures are characterized by a high surface energy, which is important for the creation of catalysts (e.g., for the ammonia and propylene oxidation).

Note that  $T_S = 900 \div 1200$  K is an optimum temperature interval for the formation of an oxide nanolayer on the Mo(110) surface in the oxygen atmosphere, because the chemical reaction rate is affected by the diffusion coefficients of oxygen and molybdenum atoms. The activation energy of the oxygen atom diffusion into the subsurface layer depends on

the packing density at the metal surface. Therefore, the formation and the desorption of  $\text{MeO}_2$ ,  $\text{MeO}_3$ , and  $(\text{MeO}_3)_2$  are observed for polycrystalline specimens or rough surfaces of molybdenum and tungsten, whereas the formation and the desorption of  $\text{MeO}$ ,  $\text{MeO}_2$ , and  $\text{MeO}_3$  are observed for the (110) facet of corresponding single crystals.

The rate of oxide formation on the surface increases, as the substrate temperature grows to 1250 K. At higher specimen temperatures ( $T_S > 1300$  K), the formation of molybdenum oxides is accompanied by their evaporation into the gas phase. As the temperature increases to 2000 K, the corrosive destruction of the surface takes place at any contact with oxygen, which is testified by the intensive evaporation of  $\text{MoO}$  from the surface, rather than its further oxidation to a more thermodynamically beneficial degree,  $\text{Mo}^{+6}\text{O}_3^{-2}$ . Therefore, in order to reduce the corrosion rate, it is expedient that molybdenum admixtures should be used in heat-resistant metallic and composite materials intended for the application at temperatures below 1300 K. The corrosion of molybdenum has to be taken into account, while creating thermal protective panels for space vehicles, because the rates of oxide formation and evaporation, in the presence of oxygen, intensively grows at temperatures above 1600 K.

From the practical viewpoint, the results obtained are also important for the development of strong contact soldering metal–ceramics [30], in particular, for hermetic connections in the space instrument engineering. The formed oxide molecules can possess non-saturated chemical bonds, which are able to create strong ionic bonds with ceramics (e.g.,  $\text{Al}_2\text{O}_3$ ,  $\text{MgO}$ , and  $\text{BaTiO}_3$ ).

*The authors express their sincere gratitude to V.I. Styopkin for his participation in the measurements and to O.G. Fedorus for the discussion of the results obtained.*

1. O. Merdrignac-Conanec and P.T. Moseley, *J. Mater. Chem.* **12**, 1779 (2002).
2. J. Meyer, A. Kröger, M. Shu *et al.*, *Appl. Phys. Lett.* **96**, 13308 (2010).
3. J. Gustafson, A. Mikkelsen, and M. Borg, *Phys. Rev. Lett.* **92**, 126102 (2004).
4. J. Gustafson, A. Mikkelsen, and M. Borg, *Phys. Rev. B* **71**, 115442 (2005).

5. A. Okada, M. Yoshimura, and K. Ueda, *Surf. Sci.* **601**, 1333 (2007).
6. K. Radican, N. Berdunov, and G. Manai, *Phys. Rev. B* **75**, 155434 (2007).
7. Y. Gotoh and E. Yanokura, *Surf. Sci.* **287/288**, 979 (1993).
8. K. Radican, S.I. Bozhko, and I.V. Shvets, *Surf. Sci.* **604**, 1548 (2010).
9. K. Reuter and M. Scheffler, *Appl. Phys. A* **78**, 793 (2004).
10. C. Dri, C. Africh, and F. Esch, *J. Chem. Phys.* **125**, 094701 (2006).
11. N.P. Vas'ko, Yu.G. Ptushinskii, and B.A. Chuikov, *Surf. Sci.* **14**, 448 (1969).
12. N.P. Vas'ko and Yu.G. Ptushinskii, *Ukr. Fiz. Zh.* **13**, 344 (1968).
13. N.P. Vas'ko and Yu.G. Ptushinskii, *Ukr. Fiz. Zh.* **13**, 1733 (1968).
14. V.A. Ishchuk, M.I. Makhkamov, and Yu.G. Ptushinskii, *Kinet. Katal.* **31**, 306 (1990).
15. N.V. Petrova and I.N. Yakovkin, *Phys. Rev. B* **76**, 205401 (2007).
16. H.M. Kennett and A.E. Lee, *Surf. Sci.* **48**, 591 (1975); **48**, 606 (1975); **48**, 617 (1975); **48**, 624 (1975); **48**, 633 (1975).
17. V.D. Osovskii, D.Yu. Balakin, and Yu.G. Ptushinskii, *Metallfiz. Noveish. Tekhnol.* **33**, 105 (2011).
18. M.L. Colaianni, J.G. Chen, and W.H. Weinberg, *Surf. Sci.* **279**, 211 (1992).
19. V.D. Osovskii, D.Yu. Balakin, and Yu.G. Ptushinskii, *Ukr. Fiz. Zh.* **54**, 1220 (2009).
20. Yu.G. Ptushinskii, *Low Temp. Phys.* **30**, 1 (2004).
21. Y.G. Zhou, X.T. Zu, J.L. Nie *et al.*, *J. Eur. Phys. B.* **67**, 27 (2009).
22. A. Kiejna and R.M. Nieminen, *J. Chem. Phys.* **122**, 044712 (2005).
23. I.N. Yakovkin, *Surf. Sci.* **577**, 229 (2005).
24. J.B. Berkowitz-Mattuck, A. Buchler, and J.E. Engelke, *J. Chem. Phys.* **39**, 2722 (1963).
25. J.C. Butty and R.E. Stickney, *J. Chem. Phys.* **51**, 4475 (1969).
26. Yu.G. Ptushinskii, B.A. Chuikov, V.D. Osovskii, and V.G. Sukretnyi, *Fiz. Nizk. Temp.* **19**, 570 (1993).
27. P.A. Redhead, *Vacuum* **12**, 203 (1962).
28. Yu.N. Kryn'ko, P.V. Mel'nik, and N.G. Nakhodkin, *Izv. Akad. Nauk SSSR Ser. Fiz.* **40**, 2505 (1976).
29. *Scanning Electron Microscopy and X-ray Microanalysis*, edited by J.I. Goldstein, D.E. Newbury, P. Echlin, D.C. Joy, Ch. Fiori, and E. Lifshin (Plenum Press, New York, 1981).
30. Yu.V. Naidich and T.V. Sidorenko, *Adhesion and Contact Interaction of Metal Melts with Barium Titanate and Other Perovskite Materials* (Naukova Dumka, Kyiv, 2013) (in Russian).

Received 30.10.2014.

Translated from Ukrainian by O.I. Voitenko

Д.Ю. Балакін, Ю.Г. Птушинський

РОЛЬ УТВОРЕННЯ І ТЕРМОДЕСОРБЦІЇ  
ОКСИДІВ МОЛІБДЕНУ В КОРОЗІЙНОМУ  
РУЙНУВАННІ ПОВЕРХНІ (110) Мо

Резюме

Експериментально досліджено адсорбційну взаємодію молекул кисню з поверхнею монокристала молібдену (110) при високих температурах. Одержано спектри термодесорбції та оже-електронів для оксидів молібдену. Встановлено механізм корозійного руйнування поверхні Мо(110). Показано, що найбільша ймовірність утворення оксидів при адсорбції кисню на поверхні Мо(110) досягається при температурі зразка 1200 К, а подальше підвищення температури стимулює процес десорбції оксидів, наслідком якого є корозія.